

Original Article

Identification of the Semangko Fault in Sumatra, Indonesia, based on gradient gravity data analysis

Muh Sarkowi, Rahmi Mulyasari, I Gede Boy Darmawan, and Rahmat Catur Wibowo*

*Department of Geophysics Engineering, Faculty of Engineering,
Universitas Lampung, Bandar Lampung, 35145 Indonesia*

Received: 12 April 2022; Revised: 6 October 2022; Accepted: 13 November 2022

Abstract

The Semangko Fault (SF) is a major active fault that extends across from Aceh (in northern part) to Lampung Province (in southern part) of Sumatra Island, contributing to much deformation and high seismicity along the fault. The fault affects a pattern in the density of surrounding rocks and can be identified by the gravity method. This research aimed to determine the fault structure using gravity gradient analysis in the Lampung area. Bouguer anomalies were analyzed from satellite gravity data and gravity gradient calculation, for fault structure identification around SF. Based on the Bouguer anomalies and gravity gradient analysis (first and second-order horizontal derivatives), SF trends NW-SE. The SF is divided into two sides at the Suoh area, West and East SF sides across to Semangko Bay. That trend is confirmed with geological and topographical data analysis. These findings suggest that gravity anomaly data and horizontal gravity gradient analysis can be used to determine and identify the presence of the SF. The seismic hazard assessments can mitigate hazards to all people in the vicinity of the SF area.

Keywords: gravity gradient, hazard mitigation, Lampung, Semangko Fault

1. Introduction

The Sumatra giant fault, the Semangko Fault (SF), is located on Sumatra Island. It extends from Semangko Bay in the northwest (NW) to the southeast (SE), parallel to the plate boundary or subduction area to the west (McCaffrey, 2009). SF in the Lampung segment extends from Semangko Bay in the south to the Suoh depression in the north. The southern part of the Semangko block is divided into landscapes: the Semangko Mountains, and Ulubelu and Walima depressions. Geological research by Sieh and Natawidjaja (2000) found that the active fault in Sumatra is a single right-step dextral fault consisting of several segments. The SF system in the Semangko segment stretches from Semangko Bay to the north to the Suoh depression, for 65 km across through volcanic rocks (Ariwibowo, Muslim, Winantris, Natawidjaja & Daryono, 2017; Bellier & Sébrier, 1994). This fault forms an asymmetrical graben with a northwest-southeast orientation which has a fault escarpment

as high as 500 m, while in the north, there is a dome-shaped Suoh depression with a width of 10 km and a length of 15 km (Alif, Fattah, & Kholil, 2020; Farr *et al.*, 2007; Natawidjaja, 2018).

The SF produces much deformation and high seismicity along the fault. Major destructive earthquakes in western Lampung occurred in 1908 and 1933, and in 1994 occurred in the Kotaagung, Suoh, and Liwa areas (Naryanto, 2008). The earthquake caused enormous damage to infrastructure, and loss of life and property. Mapping the SF zone is very important, considering that the fault zone has the potential for destructive earthquakes, and many people live in the area along the SF zone. Fault zone identification is generally carried out by several methods, such as aerial photo analysis, Landsat imagery, DEM-SRTM, geological mapping, and by several geophysical methods (gravity, magnetic, magnetotelluric, seismic) (Hanafy, Aboud, & Mesbah, 2012; Martí *et al.*, 2020; Ngadenin, Subiantoro, Widana, Sutriyono, & Widito, 2012; Schulte, Lyatsky, & Bridge, 2019).

The DEM-SRTM analysis found that this fault forms an asymmetrical graben with an NW-SE orientation with a fault girder as high as 500 m in the west, while in the north, there is a dome-shaped Suoh depression with a width of

*Corresponding author

Email address: rahmat.caturwibowo@eng.unila.ac.id

10 km and 15 km length. The SE trend of the SF zone has a width of 18 km, and the northern part before the Suoh depression has 5 km width (Alif *et al.*, 2020).

In this study, an analysis of gravity data and horizontal gradient gravity was carried out to obtain the location of the SF in the Lampung segment. The research used satellite gravity data with Bouguer correction to obtain the Bouguer anomaly. Finally, the horizontal gradient analysis was carried out to obtain the location and zone of the fault.

The Sumatra Island, which is physiographically trending NW-SE, is an extension to the south of the Eurasian Plate, precisely on the western boundary of Sundaland. The position of Sumatra Island is adjacent to the boundary between the Indo-Australian and Eurasian plates. The subduction of the two plates is marked by the active Sunda arc system extending from Burma in the north to the south, where the Indo-Australian plate collides with eastern Indonesia (Hamilton, 1979).

The SF was formed due to the collision between the India-Australia and the Eurasian continental plates. This tectonic collision occurs obliquely and creates two components of the force. This force causes the India-Australia plate to be dragged under the Eurasian plate (Meltzner *et al.*, 2010). The subduction between India-Australia and Eurasian plates forms an oblique convergent pattern at an N 20° E angle. The subduction of the Indian-Australian plate accommodates the downward movement under the Eurasian plate, resulting in two force effects (downward movement and horizontal movement). The horizontal movement is reflected in the shear fault patterns that form a series of dextral wrenching structures within the Eurasian plate. The series of shear fault structures eventually formed a giant Sumatran fault known as the SF. The shift produces a weak zone that allows magma to escape during volcanism, producing a mountain range stretching to the west of Sumatra Island from Lampung to Aceh (Figure 1).

The SF position is the western side of the Mountain Volcanic-Arc line, evidenced by the many wrench faults found in the mountain range. The tensional regime affects the back-arc basin area with the force's direction perpendicular to the subduction zone. The heat flow below the surface causes this tensional regime. The compression force that produces dextral wrenching is parallel to the plate boundary and strongly influences the tensional regime of the back-arc basin. The SF is a dextral wrench fault with clockwise movement direction (da Silva, Purwoko, Siswoyo, Thamrin, & Vacquier, 1980).

The SF is an active fault on the mainland that divides Sumatra Island, starting from Semangko Bay, stretching along the Bukit Barisan Mountains to the Aceh region in the north, parallel to the plate boundary or subduction area to the west (McCaffrey, 2009).

Geological research by Sieh and Natawidjaja (2000) found that the active fault in Sumatra is a single right-step dextral fault consisting of several segments. The Sumatran fault system in the Semangko Lampung segment stretches from Semangko bay to the north to the Suoh depression along the 65 km cutting through volcanic rock (Ariwibowo *et al.*, 2017; Bellier & Sébrier, 1994). This fault forms an asymmetrical graben with a northwest-southeast orientation with a fault plane as high as 500 m, while to the north, there is a dome-shaped Suoh depression with a width of 10 km and a

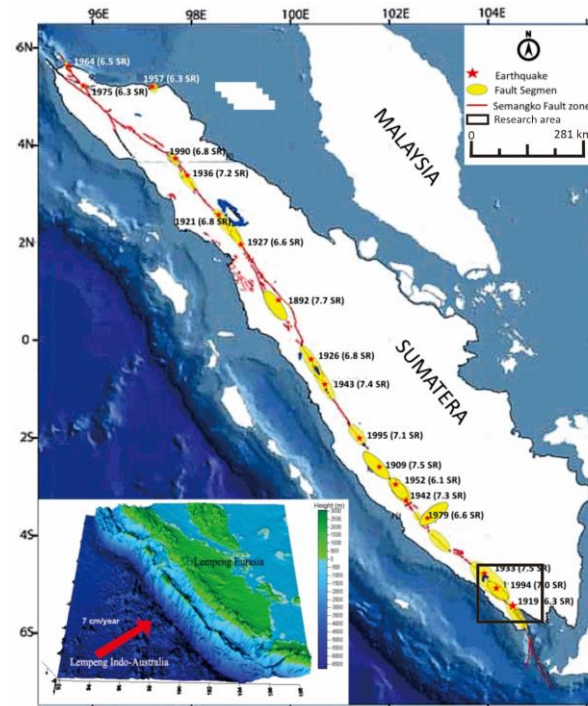


Figure 1. Indo-Australian plate collision with Eurasian, where the Indo-Australian plate subducts under the Eurasian one (modified from Sieh & Natawidjaja, 2000)

length of 15 km (Figure 2).

The regional stratigraphy of Lampung is grouped into three parts: Pre-Tertiary rock groups, including the Mount Kasih group, the Sulah complex, and the Mananga Formation. The Tertiary rock group consists of Contour Formation, and the Quaternary rock group consists of Lampung Formation, Kasai Formation, Sukadana Basalt, young volcanic deposits, and Alluvial (Mangga, Amirudin, Suwari, Gafoer, & Sidarta, 1993). The geomorphology of the western part of Lampung is divided into five units, namely lowlands, rolling hills, highlands, mountainous areas, and volcanic cones (Amin, Sidarto, Santoso, & Gunawan, 1994). The lowlands are located around the west coast of Lampung and Semangko Bay around Kota Agung. Wavy hills dominate Lampung's western part, consisting of mountains, volcanic cones, and highlands (Figure 3).

The Bukit Barisan highlands are a geanticline with a syncline located to the east. The mountain ridges from the Cretaceous were deformed during the Tertiary period, namely the occurrence of fault symptoms (vertical forces) resulting in geological phenomena such as the long SF along Way Semaka and Semangko Bay, and oval-shaped volcanoes (Tanggamus, Rindingan, Rebang and others around it). Tectonic depressions such as the Suoh, Gedong Surian, and Way Lima valleys are covered by volcanic sediments (Amin *et al.*, 1994).

The SF produces much deformation during its movement, resulting in high seismic elements along the fault (Figure 4) (Naryanto, 2008). Major destructive earthquakes in the western part of Lampung occurred in 1908, 1933 ($M = 7.5$), and 1994 ($M = 7.0$) due to earthquakes associated with the SF and originating in Kotaagung, Suoh, and Liwa areas (Natawidjaja, & Triyoso, 2007).

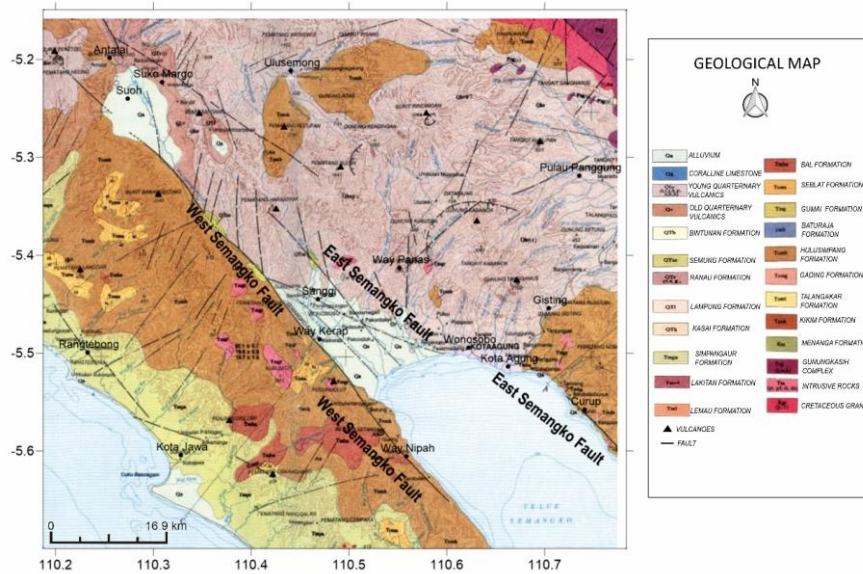


Figure 3. Stratigraphic unit of western Lampung (Amin *et al.*, 1994)

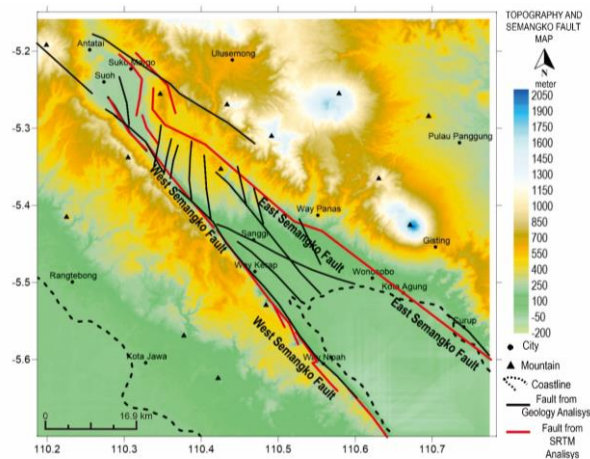


Figure 2. The SF in the research area is based on 30 m DEM-SRTM data and geological data analysis.

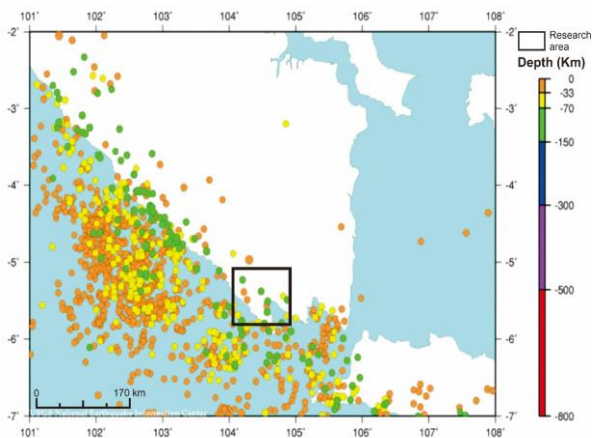


Figure 4. The epicenter of the 1990-2004 earthquake in Lampung Province and its surroundings (Naryanto, 2008)

2. Materials and Methods

The 1144 free air anomaly satellite gravity data has been used with intervals of 1800-1900 meters (https://topex.ucsd.edu/cgi-bin/get_data.cgi) to create a Bouguer anomaly map and gravity gradient analysis, and 30 m topographic data (DEM-SRTM) to produce surface structure trend pattern (<https://www.indonesia-geospasial.com/2020/01/download-dem-srtm-30-meter-se-indonesia.html>).

The data processing carried out included three main stages, namely:

- a) Data processing to obtain gravity anomaly. Data processing is carried out by calculating surface density, Bouguer correction, and calculation of gravity anomaly with Matlab. The Bouguer correction value is calculated using the infinite slab model approach (Telford, Geldart, & Sheriff, 1990):

$$B_c = 2\pi G\rho h = 0.04193\rho h$$
 where is the average rock density, which in this study was set at 2.4 g/cc, h is height (m), and B_c is the Bouguer correction (mGal).
- b) Gradient gravity analysis processing, which includes horizontal gradient gravity anomaly first order (SFHD=FHD_x+ FHD_y) and horizontal gradient gravity anomaly second-order (SSHHD=SHD_x+ SHD_y) (Sumintadireja, Dahrin, & Grandis, 2018; Sarkowi & Wibowo, 2021b; Sarkowi & Wibowo, 2021a; Sarkowi, Wibowo, & Karyanto, 2021).

- Calculation of the first-order horizontal gradient gravity anomaly was done using the equation:

$$SFHD = FHD_x + FHD_y$$

with: $FHD_x = \frac{\Delta g}{\Delta x} = \frac{g_2 - g_1}{x_2 - x_1}$ and

$$FHD_y = \frac{\Delta g}{\Delta y} = \frac{g_2 - g_1}{y_2 - y_1}$$

- Calculation of the second-order horizontal gradient gravity anomaly was done using the equation:

$$\begin{aligned} \text{SSHD} &= \text{SHD}_x + \text{SHD}_y \\ \text{with: } \text{SHD}_x &= \frac{\text{FHD}_{x2} - \text{FHD}_{x1}}{\Delta x} \text{ and} \\ \text{SHD}_x &= \frac{\text{FHD}_{x2} - \text{FHD}_{x1}}{\Delta x} \end{aligned}$$

The equation for the number of horizontal gradients of second-order (SSHD = SHD_x + SHD_y) based on the Laplace equation is called the Second Vertical Derivative (SVD) (Saibi, Nishijima, Ehara, & Aboud, 2006; Elkins, 1951).

$$\begin{aligned} \nabla^2 \Delta g &= 0 \text{ or } \frac{\partial^2 \Delta g}{\partial x^2} + \frac{\partial^2 \Delta g}{\partial y^2} + \frac{\partial^2 \Delta g}{\partial z^2} = 0 \\ \frac{\partial^2 \Delta g}{\partial z^2} &= - \frac{\partial^2 \Delta g}{\partial x^2} - \frac{\partial^2 \Delta g}{\partial y^2} \end{aligned}$$

The first-order horizontal gradient of the Bouguer anomaly, the second-order horizontal gradient of the gravity anomaly, and the SVD of the gravity anomaly are filters that can be used to generate shallow anomalies and determine the structure boundaries (faults) (Al-Khafaji, 2017; Elkins, 1951; Ming *et al.*, 2021). The fault (the anomaly boundary or fault objects) is indicated by the maximum or minimum first-order horizontal gradient value and by the second-order horizontal gradient value equal to 0 (zero), and the SVD of the Bouguer anomaly equal to 0 (zero) (Sarkowi, 2010; Sarkowi & Wibowo, 2021b; Sumintadireja *et al.*, 2018).

- Interpretation and analysis. Interpretation and analysis were carried out by comparing the first-order Bouguer anomaly gradient map (SFHD=FHD_x+ FHD_y) and the second-order Bouguer anomaly horizontal gradient map (SSHD = SHD_x + SHD_y) with geological maps and fault structures along the SF zone. This analysis is expected to assess the effectiveness of gravity data and horizontal gradient analysis to identify the faults along the SF zone.

3. Results and Discussion

The Bouguer anomaly in the study area has a value from 15 to 115 mGal, showing a dominant contour trending southeast-northwest according to the geological structure pattern of the SF. The high anomaly is in the southwest SF zone (Pematang Cawang Harjo, Pematang Luwi, and Pematang Langgar), with an anomaly trending southeast-northwest. The low anomaly is along the SF, especially in the north and northeast (Figure 5).

To support the Bouguer anomaly analysis in identifying fault structures and lithological boundaries and to generate shallow effect anomalies, a vertical gradient analysis of the Bouguer anomaly was performed. Theoretically, the horizontal gradient method of the Bouguer anomaly is the derivative of the Bouguer anomaly for the horizontal direction, which can be written as: first-order horizontal gradient in x = $\text{FHD}_x = \frac{\Delta g}{\Delta x}$ and first-order horizontal gradient in y = $\text{FHD}_y = \frac{\Delta g}{\Delta y}$. The second-order horizontal gradient in x = $\text{SHD}_x = \frac{\Delta^2 g}{\Delta x^2}$ and a second-order horizontal gradient in the y-

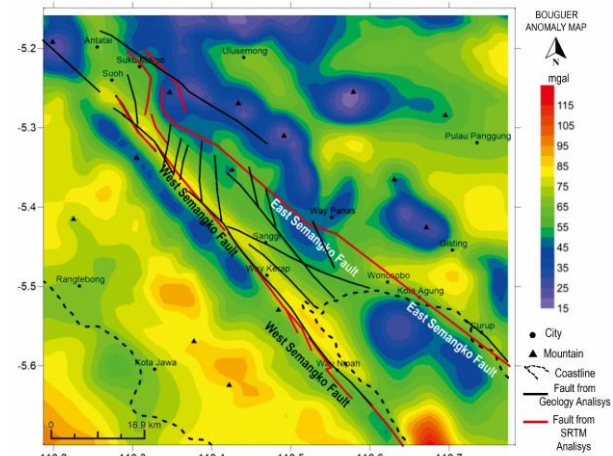


Figure 5. Bouguer anomaly map and faults based on geological maps and SRTM analysis along the SF zone from the Suoh depression to Semangko Bay.

$$\text{direction is } y = \text{SHD}_y = \frac{\Delta^2 g}{\Delta y^2}$$

In general, the existence of fault structures, intrusions, lithological boundaries, and boundary models of anomaly objects are not always in the x or y direction, so the horizontal gradient analysis uses the sum of the horizontal gradients in the x and y directions. In this research, we analyze the sum of the horizontal gradients of first-order (SFHD=FHD_x+FHD_y) and the sum of the horizontal gradients of second-order (SSHD=SHD_x+SHD_y). Identification of fault structures, intrusions, lithological boundaries, and model boundaries of anomalous bodies is indicated by the horizontal gradient value of the minimum or maximum order Bouguer anomaly and the horizontal gradient value of the Bouguer anomaly of second-order = 0 (Sarkowi, 2010; Sarkowi & Wibowo, 2021b; Sumintadireja *et al.*, 2018).

The first-order horizontal gradient anomaly map (SFHD=FHD_x+ FHD_y) has a dominant anomaly contour pattern with a NE-SW direction according to the structural direction of the SF (Figure 6). The maximum or minimum contour value indicates a fault structure or lithological boundary from the first-order horizontal gradient anomaly map (SFHD=FHD_x+ FHD_y). From the horizontal gradient anomaly of first-order (SFHD=FHD_x+ FHD_y), the presence of the SF in the West segment corresponds to the maximum contour and the SF in the East segment.

The second-order horizontal gradient anomaly map (SSHD=SHD_x+SHD_y) has a dominant anomaly contour pattern with a NE-SW direction according to the structural direction of the SF (Figure 7). The presence of fault structures or lithological boundaries from the second-order horizontal gradient anomaly map (SSHD=SHD_x+SHD_y) is indicated by 0 (zero). The horizontal gradient anomaly of second-order (SSHD=SHD_x+SHD_y) shows the presence of the West segment of the SF, which corresponds to the 0 (zero) contour of the anomaly of the SF East segment.

The topographic map of 30 m DEM-SRTM data and contour map of the second horizontal derivative anomaly gravity (SHD_x+SHD_y = 0) and the presence of the SF due to geological and DEM-SRTM analysis along the SF zone from the Suoh depression are shown in Figure 8. The map shows

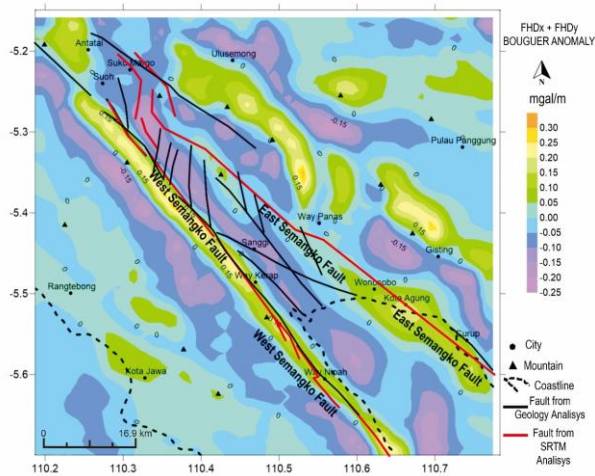


Figure 6. Horizontal gradient map of first-order gravity anomaly (FHDx + FHDy) and fault conditions based on geological maps and DEM-SRTM analysis.

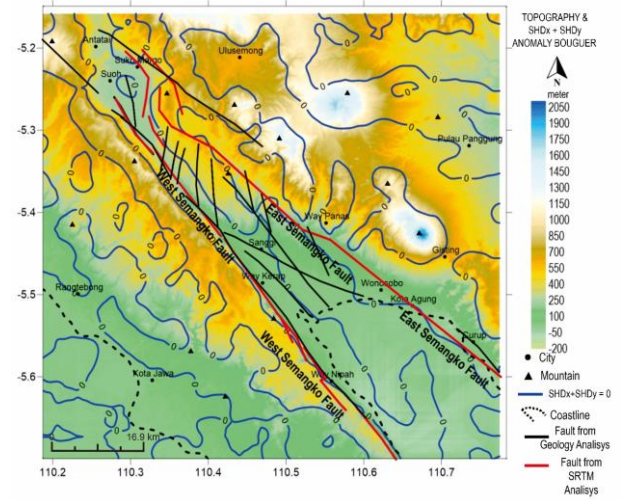


Figure 8. Topographic map of 30 m DEM-SRTM data and contour map of the second horizontal derivative of Bouguer anomaly (SHDx+SHDy = 0) and the presence of the Semangko Fault as a result of geological and DEM-SRTM analysis

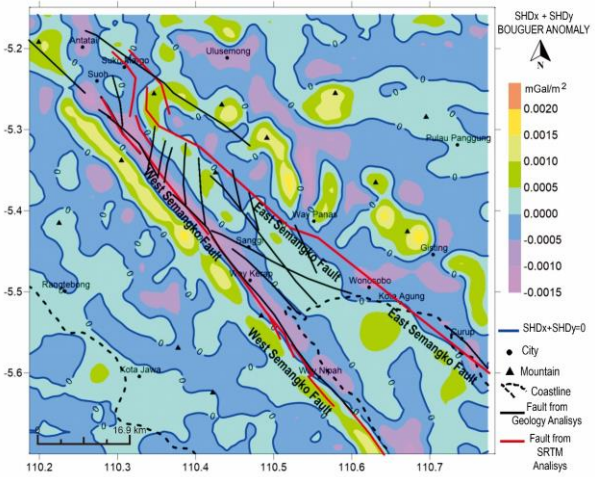


Figure 7. Horizontal gradient map of second-order gravity anomaly (SHDx + SHDy) and fault conditions based on geological maps and DEM-SRTM analysis.

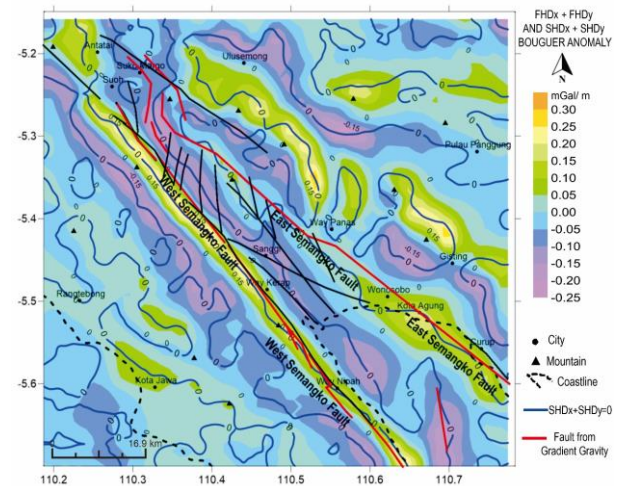


Figure 9. Comparison map between the total first-order gradient gravity anomaly of first-order (SFHD=FHDx+FHDy) and the total horizontal gradient of the second-order gravity anomaly (SSHd=SHDx+SHDy)

that the SF's western part correlates with the second horizontal derivative anomaly gravity contour ($SHD_x+SHD_y = 0$), especially in the southern part. In contrast, for the northern part, the second horizontal derivative anomaly Bouguer contour ($SHD_x+SHD_y = 0$) is correlated with the peak of the fault zone while fault from DEM-SRTM 30m and geology is in the lower fault zone.

The comparison map between the total first-order horizontal gradient gravity anomaly and the total second-order horizontal gradient gravity anomaly is shown in Figure 9. Based on Figure 9, an analysis of faults around the fault zone has been carried out. The fault boundary change is indicated by the value of the first-order horizontal gradient of the gravity anomaly maximum or minimum. The second-order horizontal gradient value of the gravity anomaly equals 0 (zero). The West segment of the SF has a straight and continuous pattern trending southeast-northwest. On the West side of the West SF, several minor faults appear in a relatively

perpendicular direction and minor faults parallel to the SF. This fault follows previous results of researchers (Alif *et al.*, 2020; Amin *et al.*, 1994; Natawidjaja, 2018).

This research can update a comprehension of the modern map of an active fault zone, especially the SF around the Lampung area, based on gravity data. However, geological activity still controls the seismicity and hence future earthquakes. Therefore, we must consider the potential hazards in this area associated with surface faultings, such as landslides and liquefaction.

4. Conclusions

The gravity anomaly along the SF from the Semangko Bay to the Suah depression has an anomalous

pattern forming a dominant contour trending NW-SE. In contrast, the gravity anomaly area in the Suoh depression area forms a circular contour pattern. The first-order gradient horizontal gradient map shows the maximum and minimum gravity gradient contours in the same location as the 0 (zero) second-order horizontal gravity gradient contour identified as a fault in the area. The analysis of gravity anomaly maps and gravity gradient indicated the presence of the West segment of SF. The pattern of the SF structure is suitable for results of geological analysis and DEM-SRTM data. These results indicate that gravity anomaly map and gradient data analysis successfully determine and identify the SF, both the western and eastern segment of the SF, around the Lampung area. Future research can pursue geophysical methods to identify a landslide and liquefaction to anticipate surface structure hazards, such as electrical resistivity tomography and HVSR. Likewise, ground-shaking hazards with deterministic and probabilistic seismic hazard assessments can mitigate hazards to all people in the vicinity of the SF area.

Acknowledgements

We want to thank all those who have helped implement this article, especially the LPPM Universitas Lampung that funded this research and Geophysics Engineering Department Universitas Lampung, where all the data was processed.

References

- Alif, S. M., Fattah, E. I., & Kholil, M. (2020). Geodetic slip rate and locking depth of east semangko fault derived from gps measurement. *Geodesy and Geodynamics*, 11(3), 222–228. doi:10.1016/j.geog.2020.04.002
- Al-Khafaji, W. M. S. (2017). Gravity field interpretation for major fault depth detection in a region located sw-qa'im/iraq. *Baghdad Science Journal*, 14(3), 625–636. doi:10.21123/bsj.2017.14.3.0625
- Amin, T. C., Sidarto, S., Santoso, & Gunawan, W. (1994). *Peta geologi lembar kotaagung, sumatera, skala 1:250.000*.
- Ariwibowo, S., Muslim, D., Winantris, Natawidjaja, D. H., & Daryono, M. R. (2017). Sub-segmentasi sesar pada segmen kumering antara danau ranau hingga lembah suoh, lampung barat. *Journal of Environment and Geological Hazard*, 8(692), 31–45.
- Bellier, O., & Sébrier, M. (1994). Relationship between tectonism and volcanism along the great sumatran fault zone deduced by spot image analyses. *Tectonophysics*, 233(3), 215–231. doi:10.1016/0040-1951(94)90242-9
- da Silva, C. H., Purwoko, Siswoyo, Thamrin, M., & Vacquier, V. (1980). Terrestrial heat flow in the tertiary basin of central sumatra. *Tectonophysics*, 69(1), 163–188. doi:10.1016/0040-1951(80)90132-8
- Elkins, T. A. (1951). The second derivative method of gravity interpretation. *Geophysics*, 16(1), 29–50. doi:10.1190/1.1437648
- Farr, T. G., Rosen, P. A., Caro, E., Crippen, R., Duren, R., Hensley, S., . . . Alsdorf, D. (2007). The shuttle radar topography mission. *Reviews of Geophysics*, 45(2). doi:10.1029/2005RG000183
- Hamilton, W. B. (1979). Tectonics of the Indonesian region. *Professional Paper*. doi:10.3133/pp1078
- Hanafy, S. M., Aboud, E., & Mesbah, H. S. A. (2012). Detection of subsurface faults with seismic and magnetic methods. *Arabian Journal of Geosciences*, 5(5), 1163–1172. doi:10.1007/s12517-010-0255-6
- Mangga, S. A., Amirudin, Suwarti, T., Gafoer, S., & Sidarta. (1993). *Peta geologi lembar tanjungkarang, sumatera, skala 1:250.000*.
- Martí, A., Queralt, P., Marcuello, A., Ledo, J., Rodríguez-Escudero, E., Martínez-Díaz, J. J., . . . Meqbel, N. (2020). Magnetotelluric characterization of the alhama de murcia fault (eastern betics, Spain) and study of magnetotelluric interstation impedance inversion. *Earth, Planets and Space*, 72(1), 16. doi:10.1186/s40623-020-1143-2
- McCaffrey, R. (2009). The tectonic framework of the sumatran subduction zone. *Annual Review of Earth and Planetary Sciences*, 37(1), 345–366. doi:10.1146/annurev.earth.031208.100212
- Meltzner, A. J., Sieh, K., Chiang, H.-W., Shen, C.-C., Suwargadi, B. W., Natawidjaja, D. H., . . . Galetzka, J. (2010). Coral evidence for earthquake recurrence and an ad 1390–1455 cluster at the south end of the 2004 aceh–andaman rupture. *Journal of Geophysical Research: Solid Earth*, 115(B10). doi:10.1029/2010JB007499
- Ming, Y., Niu, X., Xie, X., Han, Z., Li, Q., & Sun, S. (2021). Application of gravity exploration in urban active fault detection. *IOP Conference Series: Earth and Environmental Science*, 660(1). doi:10.1088/1755-1315/660/1/012057
- Naryanto, H. S. (2008). Analisis potensi kegempaan dan tsunami di kawasan pantai barat lampung kaitannya dengan mitigasi dan penataan kawasan. *Jurnal Sains Dan Teknologi Indonesia*, 10(2), 71–77.
- Natawidjaja, D. H. (2018). Updating active fault maps and sliprates along the sumatran fault zone, Indonesia. *IOP Conference Series: Earth and Environmental Science*, 118(1). doi:10.1088/1755-1315/118/1/012001
- Natawidjaja, D. H., & Triyoso, W. (2007). The sumatran fault zone – form source to hazard. *Journal of Earthquake and Tsunami*, 1(1), 21–47.
- Ngadenin, Subiantoro, L., Widana, K. S., Sutriyono, A., & Widito, P. (2012). Pemetaan geologi dan identifikasi keberadaan sesar di lokasi calon tapak pltn ketapang dan sekitarnya, madura. *Eksplorium*, 33(1), 1–14.
- Saibi, H., Nishijima, J., Ehara, S., & Aboud, E. (2006). Integrated gradient interpretation techniques for 2d and 3d gravity data interpretation. *Earth, Planets and Space*, 58(7), 815–821. doi:10.1186/BF03351986
- Sarkowi, M. (2010). Identifikasi struktur daerah panasbumi ulubelu berdasarkan analisa data svd anomali bouguer. *Journal of Sains MIPA*, 16(2), 111–118.
- Sarkowi, M., & Wibowo, R. C. (2021a). Geothermal reservoir identification based on gravity data analysis in rajabasa area- lampung. *RISSET Geologi Dan Pertambangan*, 31(2), 77. doi:10.14203/rissetgeotam2021.v31.1164

- Sarkowi, M., & Wibowo, R. C. (2021b). Reservoir identification of bac-man geothermal field based on gravity anomaly analysis and modeling. *Journal of Applied Science and Engineering*, 25(2), 329–338. doi:10.6180/jase.202204_25(2).0009 1.
- Sarkowi, M., Wibowo, R. C., & Karyanto. (2021). Geothermal reservoir identification in way ratai area based on gravity data analysis. *Journal of Physics: Conference Series*, 2110(1). doi:10.1088/1742-6596/2110/1/012004
- Schulte, B. W. M. P. G., lyatsky, H., & Bridge, D. (2019). Methods of fault detection with geophysical data and surface geology. *Canadian Journal of Exploration Geophysics*, 44(5), 1–23.
- Sieh, K., & Natawidjaja, D. H. (2000). Neotectonics of the sumatran fault, indonesia. *Journal of Geophysical Research*, 105(B12), 31. doi:10.1029/2000JB900120
- Sumintadireja, P., Dahrin, D., & Grandis, H. (2018). A note on the use of the second vertical derivative (svd) of gravity data with reference to indonesian cases. *Journal Engineering, Technology, and Science*, 50(1), 127–139. doi:10.5614/j.eng.technol.sci.2018.50.1.9
- Telford, W. M., Geldart, L. P., & Sheriff, R. E. (1990). *Applied geophysics: second edition*. New York, NY: Cambridge University Press.